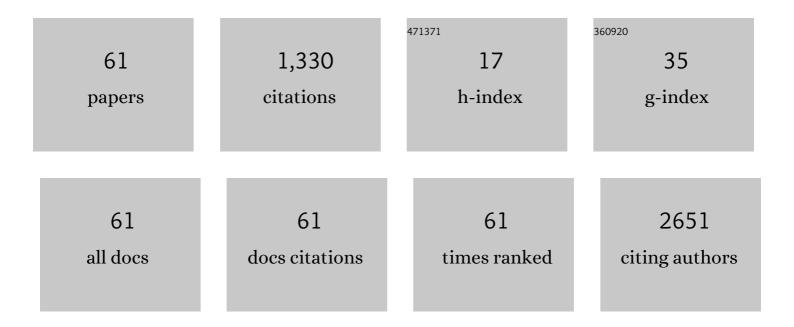
Anupam Roy

List of Publications by Year in descending order

Source: https://exaly.com/author-pdf/7758757/publications.pdf Version: 2024-02-01



ANUDAM ROY

#	Article	IF	CITATIONS
1	Devices and defects in two-dimensional materials: outlook and perspectives. , 2022, , 339-401.		1
2	Wafer-Scalable Single-Layer Amorphous Molybdenum Trioxide. ACS Nano, 2022, 16, 3756-3767.	7.3	16
3	Silicon nanodots via sputtering of Si(111)-7×7 surfaces and post-annealing. Materials Today: Proceedings, 2021, 47, 1617-1620.	0.9	0
4	Two-Step Growth of Uniform Monolayer MoS ₂ Nanosheets by Metal–Organic Chemical Vapor Deposition. ACS Omega, 2021, 6, 10343-10351.	1.6	14
5	Direct growth of <mml:math xmlns:mml="http://www.w3.org/1998/Math/MathML"> <mml:msub> <mml:mi> MoS </mml:mi> <mml:mn>2 on electrolytic substrate and realization of high-mobility transistors. Physical Review Materials, 2021, 5</mml:mn></mml:msub></mml:math 	l:mŋ>៹/m	ml:msub>
6	Recent progress on measurement of spin–charge interconversion in topological insulators using ferromagnetic resonance. APL Materials, 2021, 9, .	2.2	7
7	Intermediate Cu-O-Si Phase in the Cu-SiO ₂ /Si(111) System: Growth, Elemental, and Electrical Studies. ACS Omega, 2021, 6, 23826-23836.	1.6	8
8	Nonpolar Resistive Switching of Multilayerâ€hBNâ€Based Memories. Advanced Electronic Materials, 2020, 6, 1900979.	2.6	42
9	Two-Dimensional to Three-Dimensional Growth of Transition Metal Diselenides by Chemical Vapor Deposition: Interplay between Fractal, Dendritic, and Compact Morphologies. ACS Applied Materials & Interfaces, 2020, 12, 15885-15892.	4.0	20
10	Structural and magnetic properties of molecular beam epitaxy grown chromium selenide thin films. Physical Review Materials, 2020, 4, .	0.9	5
11	Growth of lateral graphene/h-BN heterostructure on copper foils by chemical vapor deposition. Nanotechnology, 2019, 30, 03LT01.	1.3	12
12	Accelerated carrier recombination by grain boundary/edge defects in MBE grown transition metal dichalcogenides. APL Materials, 2018, 6, .	2.2	25
13	Carrier Trapping by Oxygen Impurities in Molybdenum Diselenide. ACS Applied Materials & Interfaces, 2018, 10, 1125-1131.	4.0	37
14	Progress in Contact, Doping and Mobility Engineering of MoS2: An Atomically Thin 2D Semiconductor. Crystals, 2018, 8, 316.	1.0	118
15	Evidence of Formation of Superdense Nonmagnetic Cobalt. Scientific Reports, 2017, 7, 41856.	1.6	10
16	Detection of current induced spin polarization in epitaxial Bi2Te3 thin film. Applied Physics Letters, 2017, 110, .	1.5	3
17	Angular dependence of magnetization reversal in epitaxial chromium telluride thin films with perpendicular magnetic anisotropy. Journal of Magnetism and Magnetic Materials, 2017, 437, 72-77.	1.0	21
18	Short-Term Relaxation in HfO _{<italic>x</italic>} /CeO _{<italic>x</italic>} Resistive Random Access Memory With Selector. IEEE Electron Device Letters, 2017, 38, 871-874.	2.2	16

ANUPAM ROY

#	Article	IF	CITATIONS
19	Intra-domain periodic defects in monolayer MoS2. Applied Physics Letters, 2017, 110, .	1.5	16
20	Laser Spike Annealing for Shallow Junctions in Ge CMOS. IEEE Transactions on Electron Devices, 2017, 64, 346-352.	1.6	13
21	Tailored MoS ₂ nanorods: a simple microwave assisted synthesis. Materials Research Express, 2017, 4, 115012.	0.8	25
22	Experimental evidence of exciton capture by mid-gap defects in CVD grown monolayer MoSe2. Npj 2D Materials and Applications, 2017, 1, .	3.9	56
23	Versatile Large-Area Custom-Feature van der Waals Epitaxy of Topological Insulators. ACS Nano, 2017, 11, 7457-7467.	7.3	6
24	A sub-1-volt analog metal oxide memristive-based synaptic device with large conductance change for energy-efficient spike-based computing systems. Applied Physics Letters, 2016, 109, .	1.5	63
25	Localization and interaction effects of epitaxial Bi ₂ Se ₃ bulk states in two-dimensional limit. Journal of Applied Physics, 2016, 120, 164301.	1.1	9
26	Large area chemical vapor deposition growth of monolayer MoSe ₂ and its controlled sulfurization to MoS ₂ . Journal of Materials Research, 2016, 31, 917-922.	1.2	14
27	Nanoscale doping of compound semiconductors by solid phase dopant diffusion. Applied Physics Letters, 2016, 108, 122107.	1.5	1
28	First-principles simulation of oxygen vacancy migration in \$\$hbox {HfO}_{ x}\$\$, \$\$hbox {CeO}_{ x}\$\$, and at their interfaces for applications in resistive random-access memories. Journal of Computational Electronics, 2016, 15, 741-748.	1.3	2
29	Structural and Electrical Properties of MoTe ₂ and MoSe ₂ Grown by Molecular Beam Epitaxy. ACS Applied Materials & Interfaces, 2016, 8, 7396-7402.	4.0	189
30	Characteristics and mechanism study of cerium oxide based random access memories. Applied Physics Letters, 2015, 106, .	1.5	37
31	Cerium oxide based bipolar resistive switching memory with low operation voltage and high resistance ratio. , 2015, , .		1
32	Air Stable Doping and Intrinsic Mobility Enhancement in Monolayer Molybdenum Disulfide by Amorphous Titanium Suboxide Encapsulation. Nano Letters, 2015, 15, 4329-4336.	4.5	167
33	Perpendicular Magnetic Anisotropy and Spin Glass-like Behavior in Molecular Beam Epitaxy Grown Chromium Telluride Thin Films. ACS Nano, 2015, 9, 3772-3779.	7.3	70
34	Strong spin-orbit coupling and Zeeman spin splitting in angle dependent magnetoresistance of Bi2Te3. Applied Physics Letters, 2014, 104, .	1.5	29
35	Thin, relaxed Si1â^'xGex virtual substrates on Si grown using C-doped Ge buffers. Applied Physics Letters, 2014, 105, 152107.	1.5	0
36	Self-organized trench–island structures in epitaxial cobalt silicide growth on Si(111). Surface Science, 2014, 620, 23-29.	0.8	7

ANUPAM ROY

#	Article	IF	CITATIONS
37	The effect of exclusion on nonlinear reaction–diffusion system in inhomogeneous media. Physica A: Statistical Mechanics and Its Applications, 2014, 405, 52-62.	1.2	1
38	Two-dimensional weak anti-localization in Bi2Te3 thin film grown on Si(111)-(7 × 7) surface by molecu beam epitaxy. Applied Physics Letters, 2013, 102, .	lar 1.5	72
39	Uniformity of epitaxial nanostructures of CoSi2 via defect control of the Si (111) surface. Thin Solid Films, 2013, 534, 296-300.	0.8	8
40	Self-organized one-atom thick fractal nanoclusters via field-induced atomic transport. Journal of Applied Physics, 2013, 114, 064304.	1.1	8
41	Negative differential resistance in electron tunneling in ultrathin films near the two-dimensional limit. Journal of Applied Physics, 2013, 113, 034308.	1.1	8
42	Nanodot to nanowire: A strain-driven shape transition in self-organized endotaxial CoSi2 on Si(100). Applied Physics Letters, 2012, 100, .	1.5	27
43	A reaction diffusion model of pattern formation in clustering of adatoms on silicon surfaces. AIP Advances, 2012, 2, 042101.	0.6	4
44	Patterns in Ge cluster growth on clean and oxidized Si(111)-(7×7) surfaces. Surface Science, 2012, 606, 777-783.	0.8	12
45	Growth of epitaxially oriented Ag nanoislands on air-oxidized Si(111)-(7×7) surfaces: Influence of short-range order on the substrate. Applied Surface Science, 2012, 258, 2255-2265.	3.1	4
46	Epitaxyâ€like orientation of nanoscale Ag islands grown on airâ€oxidized Si(110)â€(5 × 1) surfaces. Su and Interface Analysis, 2012, 44, 513-518.	ırfaçe 0.8	1
47	Fractal pattern formation in thermal grooving at grain boundaries in Ag films on Si(111) surfaces. Thin Solid Films, 2012, 520, 5086-5090.	0.8	12
48	Growth of oriented Ag nanocrystals on air-oxidized Si surfaces: An in-situ reflection high energy electron diffraction study. Thin Solid Films, 2011, 520, 853-860.	0.8	4
49	Lateral straggling and its influence on lateral diffusion in implantation with a focused ion beam. Nuclear Instruments & Methods in Physics Research B, 2011, 269, 856-860.	0.6	2
50	Growth mechanisms for wire-like epitaxial gold silicide islands on Si(110) surfaces. Applied Surface Science, 2011, 257, 3248-3252.	3.1	11
51	Desorption of Ag from Grain Boundaries in Ag Film on Br and H-Passivated Si(111) Surfaces. , 2011, , .		1
52	Self-organized Growth of Cobalt Nanostructures on Agâ^•Si (111)-7×7 Surfaces. , 2011, , .		0
53	Formation of aligned nanosilicide structures in a MBE-grown Au/Si(110) system: a real-time temperature-dependent TEM study. Journal of Physics Condensed Matter, 2009, 21, 205403.	0.7	14
54	Growth of (â^š3×â^š3)-Ag and (111) oriented Ag islands on Ge/Si(111) surfaces. Applied Surface Science, 2009, 256, 508-512.	3.1	8

4

ANUPAM ROY

#	Article	IF	CITATIONS
55	Ultrasmall Ge islands with low diameter-to-height aspect ratio on Si(100)-(2×1) surfaces. Applied Surface Science, 2009, 256, 356-360.	3.1	2
56	Estimation of diffusion coefficient by photoemission electron microscopy in ion-implanted nanostructures. Applied Surface Science, 2009, 256, 536-540.	3.1	10
57	Growth of oriented crystalline Ag nanoislands on air-exposed Si(001) surfaces. Applied Surface Science, 2009, 256, 361-364.	3.1	8
58	Ge growth on self-affine fractal Si surfaces: influence of surface roughness. Journal Physics D: Applied Physics, 2009, 42, 145303.	1.3	10
59	Surface roughness of ion-bombarded Si(100) surfaces: Roughening and smoothing with the same roughness exponent. Nuclear Instruments & Methods in Physics Research B, 2008, 266, 1276-1281.	0.6	17
60	Electronic structure of Ag-adsorbed nanowire-like stripes onSi(110)â^'(16×2)surfaces. I. Anin situSTM and STS experiment. Physical Review B, 2008, 77, .	1.1	11
61	Electronic structure of Ag-adsorbed nanowire-like stripes onSi(110)â^'(16×2)surfaces. II. A one-dimensional tight-binding model with Green's function approach. Physical Review B, 2008, 77, .	1.1	3